ELSEVIER

Journal of Alloys and Compounds 450 (2008) 521–524

Journal of ALLOYS AND COMPOUNDS

www.elsevier.com/locate/jallcom

Low-temperature growth and optical properties of ZnO nanorods

Jinghai Yang [a,b,*], Jihui Lang [a], Lili Yang [b,c,a], Yongjun Zhang [a], Dandan Wang [a], Hougang Fan [a], Huilian Liu [b,c,a], Yaxin Wang [a], Ming Gao [a]

[a] *The Institute of Condensed State Physics, Jilin Normal University, Siping 136000, PR China*
[b] *Key Laboratory of Excited State Processes, Changchun Institute of Optics, Fine Mechanics and Physics, Chinese Academy of Sciences, Changchun 130033, PR China*
[c] *Graduate School of the Chinese Academy of Sciences, Beijing 100049, PR China*

Received 3 December 2006; received in revised form 29 December 2006; accepted 31 December 2006
Available online 10 January 2007

Abstract

Zinc oxide (ZnO) nanorods were grown on ITO conducting glass by the chemical solution deposition method (CBD) in an aqueous solution that contained zinc nitrate hexahydrate ($Zn(NO_3)_2{\cdot}6H_2O$) and methenamine ($C_6H_{12}N_4$). The size of ZnO nanorods increased with molar concentration of zinc nitrate, and the nanorods with different aspect ratios also formed through tuning the reaction time when the molar concentration was 0.1 M. The length of nanorods increased significantly with the reaction time, but the thickness of the film deposited on the substrate only slightly increased. From the X-ray measurement results, it can be seen that the growth orientation of the as-prepared ZnO nanorods was [0 0 2]. Photoluminescence measurements were also carried out, the result showed a blue shift in violet emission with the reduction in crystal size.

Keywords: ZnO nanorods; Chemical solution deposition; Photoluminescence

1. Introduction

One-dimensional (1D) nanocrystalline semiconductors such as nanorods, nanotubes and nanowires have attracted considerable attention due to their importance in basic scientific research and potential technological application [1]. Among these materials, zinc oxide (ZnO) as a wide band gap semiconductor attracts a major intention in current semiconductor research, for its super optical properties. Due to wide band gap (3.37 eV) at room temperature, ZnO becomes an excellent semiconductor material for applications considered for other wide bandgap materials like GaN and SiC. In addition, due to the extreme large exciton binding energy (60 meV), the excitons in ZnO are thermally stable at room temperature, and thus ZnO has signicant advantages in optoelectronic applications such as the ultraviolet (UV) lasing media [2]. Up to now, most physical and chemical methods are used to fabricate ZnO nanorods, such as vapor phase transport deposition, pulsed laser ablation, chemical vapor deposition, electrodeposition and thermal evaporation [3–7]. According to these methods, they are not suitable for controllable synthesis. Moreover, the complex processes, sophisticated equipment and economically prohibitive high temperatures are also required. Compared with those methods, chemical solution deposition method (CBD) can be controlled easily, and no sophisticated equipments are required. The most important is that the experiment can be carried out under low temperature. In addition, the high electrical conductivity and optical transparency of ITO conducting glass substrate used in our experiment also provide a great potential in future optoelectronic nanodevice applications. Therefore, in this paper, two series of ZnO nanorods with different morphologies are prepared by the method of CBD through adjusting the growth moral concentration of zinc nitrate and reaction time, wherein no surfactants are involved. Then their structure, morphologies and optical properties are studied.

2. Experimental

ZnO nanorods used in the experiment were grown on the ITO conducting glass by the CBD process. In the process, aqueous solution of zinc nitrate hexahydrate [$Zn(NO_3)_2{\cdot}6H_2O$, 99.9% purity] and methenamine ($C_6H_{12}N_4$, 99.9% purity) was first prepared, while keeping the same 1:1 ratio [e.g., zinc nitrate hexahydrate solution (0.1 M) and methenamine solution (0.1 M)]. Two series of samples were prepared in our experiment. One series of samples was obtained

* Corresponding author. Tel.: +86 434 3290009; fax: +86 434 3294566.
E-mail address: jhyang@jlnu.edu.cn (J. Yang).

0925-8388/$ – see front matter © 2007 Elsevier B.V. All rights reserved.
doi:10.1016/j.jallcom.2006.12.135

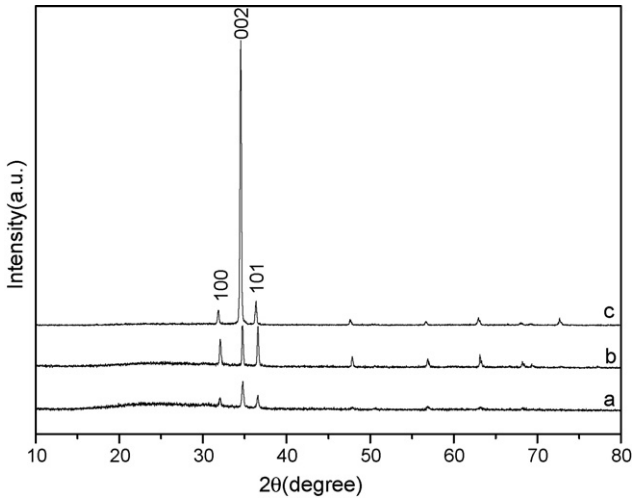

Fig. 1. XRD patterns of ZnO nanorods on the ITO conducting glass substrate in aqueous solution with different molar concentration of zinc nitrate when the reaction time is 12 h. (a) 0.01 M; (b) 0.05 M; (c) 0.1 M.

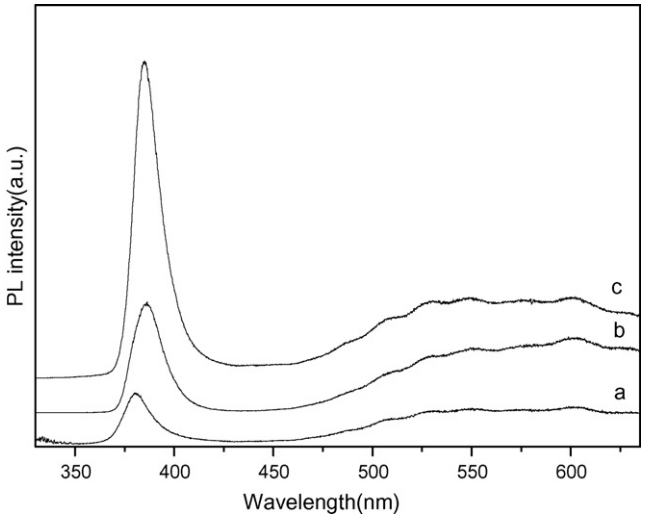

Fig. 3. PL spectra of ZnO nanorods on the ITO conducting glass substrate in aqueous solution with different molar concentration of zinc nitrate when the reaction time is 12 h. (a) 0.01 M; (b) 0.05 M; (c) 0.1 M.

when the concentration of zinc and amine were fixed at 0.01 M, 0.05 M and 0.1 M. The reaction time was 12 h. The other series was grown when the reaction time was 5 h, 12 h and 28 h, respectively. The concentration of zinc was 0.1 M.

ITO conducting glass was used as the substrates, which were cleaned ultrasonically with acetone, ethanol and deionized water for 20 min, respectively. Then, the substrates were immersed and tilted against the wall of bottle in the precursor solution at 90 °C in an oven for several hours without any stirring. Subsequently, the thin films were thoroughly cooled to room temperature, washed with deionized water and dried in air.

XRD (MAC Science, MXP18, Japan), SEM (Hitachi, S-570) and PL (He–Cd Laser, 325 nm) were used to characterize the crystal structure, surface morphologies and optical properties of ZnO nanorods.

3. Results and discussion

3.1. Effect of different molar concentration of zinc nitrate on ZnO nanorods

Fig. 1 shows the XRD patterns of ZnO nanorods deposited on the ITO conducting glass substrate with different molar ratio of zinc nitrate. From Fig. 1, it can be seen that the deposited ZnO nanorods have hexagonal wurtzite structure. In addition, [1 0 1] reflection peak is usually the maximum one in the standard pattern of ZnO, while in Fig. 1, [0 0 2] reflection peak apparently stronger than [1 0 1], which indicates that the ZnO nanorods trend to grow perpendicular to the ITO conducting glass substrate surface. That is to say, the *c*-axis is the optimum orientation of these deposited ZnO nanorods.

Fig. 2 shows the SEM images of ZnO nanorods with different concentration of zinc nitrate (Fig. 2(a)) 0.01 M, (Fig. 2(b)) 0.05 M and (Fig. 2(c)) 0.1 M, when the reaction time was fixed at 12 h. It indicated that the concentration of zinc nitrate was the important factor that governed the diameter of the nanorods, due to the critical diffusion of the monomers and subsequent limited growth [8]. Nanorods with the size of 600 nm were obtained at the concentration of 0.1 M zinc nitrate, and then nanorods about 300–400 nm at 0.05 M, as well as nanorods about 200–300 nm at 0.01 M were targeted. In general, the sizes of the ZnO nanorods become bigger with a higher concentration of zinc nitrate.

Fig. 3 illustrates the room-temperature photoluminescence (PL) spectra of ZnO nanorods grown on the ITO conducting glass substrate with different molar concentration of zinc nitrate. As seen in Fig. 3(a), three luminescence emission peaks, ultra-

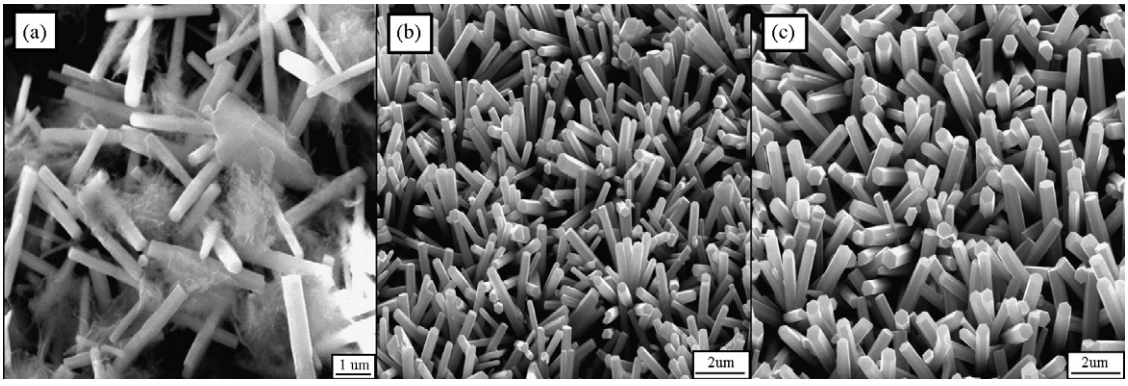

Fig. 2. SEM images of ZnO nanorods on the ITO conducting glass substrate in aqueous solution with different molar concentration of zinc nitrate when the reaction time is 12 h. (a) 0.01 M; (b) 0.05 M; (c) 0.1 M.

violet (UV) emission at 380 nm, green emission at 550 nm and yellow emission at 599 nm, were observed. Generally, the UV emission of ZnO was attributed to an exciton-related activity [9], and the green emission was due to the point defects, such as oxygen vacancies or impurities [10]. The deep level involved in the yellow luminescence was likely interstitial oxygen [11], and perhaps had much to do with the structure of ZnO_2 [12]. As the molar concentration increased to 0.05 M, the PL peak in the UV and green regions gradually increased, but the yellow emission decreased (Fig. 3(b)). As the molar concentration increased to 0.1 M, the PL peak in the green and yellow regions gradually decreased. However, the UV emission peak increased again with the increase of the molar concentration (Fig. 3(c)). It may be explained that the UV emission has much sharper peak, the samples would have more perfect crystallization.

In conclusion, when the molar concentration of zinc nitrate was fixed at 0.1 M, the structure, morphologies and optical properties of the ZnO nanorods were optimum.

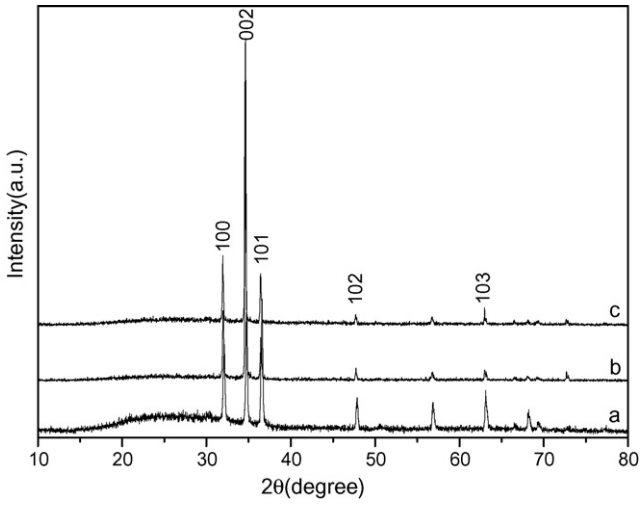

Fig. 4. XRD patterns of ZnO nanorods on the ITO conducting glass substrate in aqueous solution with different reaction time when the molar concentration of zinc nitrate is 0.1 M. (a) 5 h; (b) 12 h; (c) 28 h.

3.2. Effect of different reaction time on ZnO nanorods

Fig. 4 shows the XRD patterns of ZnO nanorods deposited on the ITO conducting glass substrate with different reaction time when the molar concentration of zinc nitrate is 0.1 M. According to the standard pattern of ZnO, all peaks in Fig. 4 can be indexed to the hexagonal wurtizite structure of zinc oxide. It can be clearly seen that no characteristic peaks of impurities are observed, and the [0 0 2] reflection is greatly enhanced relative to the usual [1 0 1] maximum reflection of ZnO zincite. The explanation is similar to Fig. 1.

Fig. 5 shows SEM images of ZnO nanorods grown on the ITO conducting glass substrate for different reaction time at 90 °C. It can be seen that the coverage density and morphologies of ZnO nanorods are significantly different. With the reaction time increasing, the diameter and length of ZnO nanorods increased. As reaction time was 5 h, the ZnO nanorod arrays were grown with diameter of ~400 nm and length of ~2.2 μm. When the reaction time further increased to 12 h, the well-aligned ZnO nanorod arrays could be obtained with diameter of ~600 nm and length of ~3.0 μm, which could be clearly shown in Fig. 5(b). Furthermore, when the reaction time increased to 28 h, the SEM images of ZnO were apparently different according to Fig. 5(c and d). It can be seen that ZnO nanotubes formed in the ZnO nanorod arrays, which was because the end of ZnO nanorods were erodent. While this kind of erosion has different effect on every ZnO nanorod, so there are three kinds of nanostructures can be seen in this image, nanorods, nanotubes, and another nanostructure of not thoroughly nanotubes with particles in them.

The formation mechanism of these nanostructures is just as follows: the CBD method consists of two steps, nucleation and growth, which is based on the formation of solid phase from the solution [13]. In the nucleation process, the clusters of molecules formed undergo rapid decomposition and particles combine to grow up to a certain thickness of the film at the ITO conducting glass substrate [14]. For our experiment, $Zn(NO_3)_2{\cdot}6H_2O$ used as the source of zinc and $C_6H_{12}N_4$ provided the OH^-. When $C_6H_{12}N_4$ was added to the solution, no precipitate occurs at once. While, with the increase of the temperature, the precipitate $Zn(OH)_2$ occurred. ZnO nuclei were formed from the precipitate deposited on the ITO substrate, and then ZnO nanorods grew from the nuclei. As the reaction time increasing, the diameter and

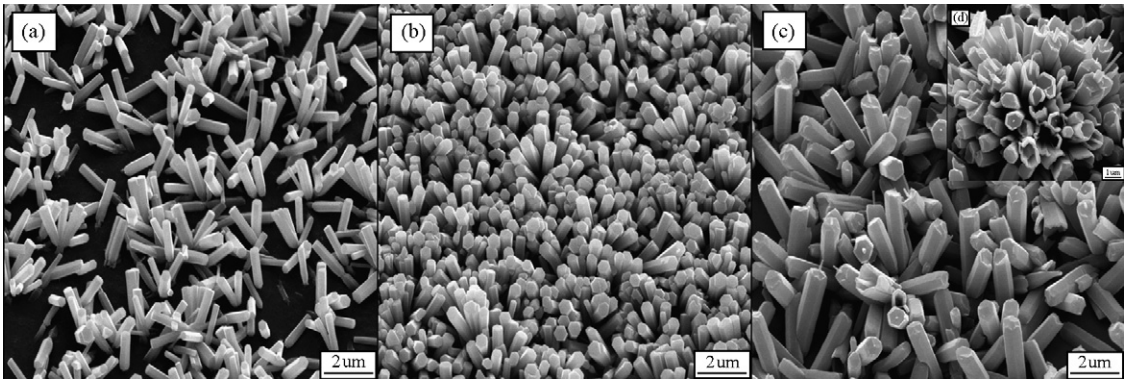

Fig. 5. SEM images of ZnO nanorods grown on the ITO conducting glass substrate in aqueous solution with different reaction time when the molar concentration of zinc nitrate is 0.1 M. (a) 5 h; (b) 12 h; (c and d) 28 h.

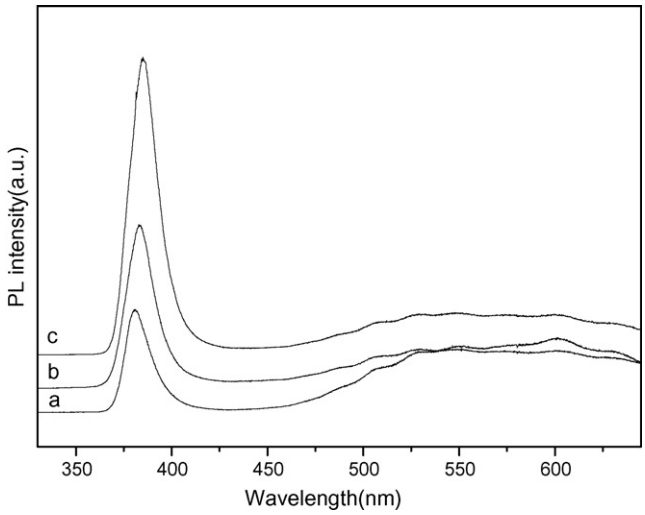

Fig. 6. PL spectra of ZnO nanorods on the ITO conducting glass substrate in aqueous solution with different reaction time when the molar concentration of zinc nitrate is 0.1 M. (a) 5 h; (b) 12 h; (c) 28 h.

length of ZnO nanorods increased. But the growth process will stop beyond a certain period of time, and subsequently the erosion process will began (Fig. 5(a–d)). In addition, the as-grown ZnO nanorod belongs to the hexagonal wurtzite type lattice, so the positive-face (0 0 0 1) and negative-face (0 0 0 $\bar{1}$) are on the metastable state; the hexagonal cylinder {0 1 $\bar{1}$ 0} is on the stable state [15]. The face on the metastable state is prone to be erosion through continual chemical reaction and then hollow nanotubes formed (Fig. 5(c and d)).

Photoluminescence (PL) of the ZnO nanorods with different reaction time were measured at room temperature and the spectra is shown in Fig. 6. In Fig. 6(a), according to the ZnO nanorods grown for a short period of time, i.e., 5 h, a weak UV emission around 381 nm and a broad green emission around 550 nm, even a weak yellow emission around 600 nm can be observed. As the ZnO nanorods were grown for 12 h, a much stronger PL emission at 383 nm and a relatively weak green emission at 550 nm, were detected (Fig. 6(b)). However, for the ZnO nanorods with a long-term growth, i.e., 28 h, some nanotubes were found in the nanorod arrays in Fig. 5(c and d). Simultaneously, only a stronger UV emission peak compared to that of ZnO nanorods grown for 5 h and 12 h is observed in Fig. 6(c). This result may be attributed to the perfect boundaries and alignment between ZnO nanorods.

In a word, when reaction time was fixed at 12 h, the structure, morphologies and optical properties of the ZnO nanorods were optimum. And from the two PL spectra as shown in Figs. 3 and 6, it can be seen that the photoluminescence measurements showed a blue shift in violet emission with the reduction in crystal size.

4. Conclusion

In summary, two series of ZnO nanorods were grown on ITO conducting glass substrate by the CBD method. Different morphologies of ZnO nanorods were obtained through adjusting the growth moral concentration and reaction time, wherein no surfactants were involved. According to both two series of samples, the XRD and SEM results indicated that *c*-axis was the optimum orientation. The size of the ZnO nanorods was smaller in a low molar concentration or a short reaction time. Photoluminescence measurements showed a blue shift in violet emission with a reduction of the molar concentration and the reaction time, that is to say, with a reduction in crystal size.

Acknowledgements

We would like to thank financial support of the program of State Key Program for Basic Research of China (grant 2003CD314702-02) and the science and technology bureau of Jilin province (Item No. 20060518) and gifted youth program of Jilin province (No. 20060123).

References

[1] X. Duan, Y. Hunag, Y. Cui, J. Wang, C.M. Lieber, Nature 409 (2001) 66; M.H. Huang, S. Mao, H. Feick, H. Yang, Y. Wu, H. Kind, E. Weber, R. Russo, P. Yang, Science 292 (2001) 1897.
[2] Q.X. Zhao, M. Willander, Appl. Phys. Lett. 83 (2003) 165–167.
[3] Y. Wu, P. Yang, Chem. Mater. 12 (2000) 605.
[4] M.H. Huang, Y. Wu, H. Feick, E. Weber, P. Yang, Adv. Mater. 13 (2001) 113.
[5] Y. Wu, R. Fan, P. Yang, Nano Lett. 2 (2002) 83.
[6] P.M. Izaki, T. Omi, J. Electrochem. Soc. 144 (1997) 1949.
[7] Z.W. Pan, Z.R. Dai, Z.L. Wang, Science 291 (2001) 1947.
[8] L. Vayssieres, Adv. Mater. 15 (2003) 464–466.
[9] D.M. Bengal, Y.F. Chen, Z. Zhu, T. Yao, Appl. Phys. Lett. 70 (1997) 2230.
[10] B.K. Choi, D.H. Chang, Y.S. Yoon, S.J. Kang, J. Mater. Sci. 10854 (2006) 9036.
[11] D. Li, Y.H. Djurisic, A.B. Leung, Z.T. Liu, M.H. Xie, S.L. Shi, S.J. Xu, W.K. Chan, Appl. Phys. Lett. 85 (2004) 1601.
[12] W.D. Yu, X.M. Li, X.D. Gao, P.S. Qiu, W.X. Cheng, A.L. Ding, Appl. Phys. A (2004) 2665.
[13] V.R. Shindea, C.D. Lokhandea, R.S. Maneb, Appl. Surf. Sci. 245 (2005) 407.
[14] X. Liu, Z. Jin, S. Bu, J. Zhao, Z. Liu, Mater. Lett. 59 (2005) 3994–3999.
[15] J. Chen, C. Guo, L. Zhang, J. Hu, P. Guo, Chin. J. Lumin. 26 (2005) 83–88.